

Cite this: *Chem. Sci.*, 2025, **16**, 15462

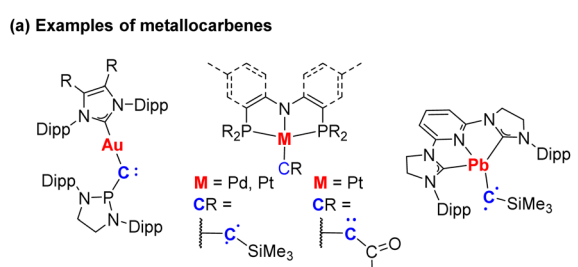
All publication charges for this article have been paid for by the Royal Society of Chemistry

Received 8th May 2025
Accepted 22nd July 2025DOI: 10.1039/d5sc03342j
rsc.li/chemical-science

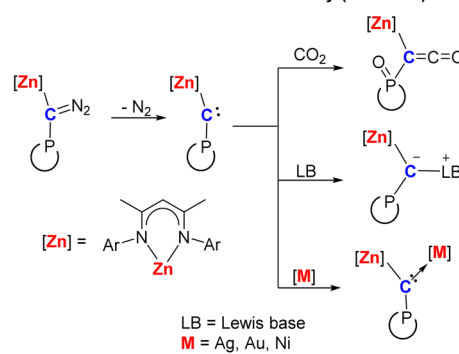
Introduction

Carbenes are compounds with a neutral divalent carbon atom. Although they have been regarded as transient intermediates for over a century, the seminal discovery of stable carbenes by Bertrand¹ and Arduengo² led to their widespread application in various fields, including catalysis, materials science, and medicinal chemistry.³ Rationally designed substituents played a crucial role in stabilizing free carbenes through steric and electronic effects.⁴ Importantly, these substituent effects govern the energetic positions of the frontier orbitals, thereby determining the reactivity of carbenes. Carbenes with metal substituents, so-called metallocarbenes, are particularly attractive as they represent the limiting configurations of metal carbynes and offer potential for diverse reactivity. However, the construction of metallocarbenes remains energetically unfavorable due to their high-energy excited-state configurations. Recently, Liu and coworkers reported the isolation of the first monometal-substituted carbenes based on the electron-rich late transition metal Au (Scheme 1a, A).⁵ In contrast, a Cu analogue

synthesized by the same group was characterized as a carbyne anion copper complex.⁶ Through the photocrystallographic technique, Schneider and coworkers obtained the Pd- and Pt-



(b) Zn-substituted carbenes and their reactivity (this work)



^aKey Laboratory of Organic Synthesis of Jiangsu Province, State Key Laboratory of Bioinspired Interfacial Materials Science, College of Chemistry, Chemical Engineering and Materials Science, Soochow University, Suzhou 215123, P. R. China. E-mail: xinxu@suda.edu.cn

^bLPCNO, CNRS, INSA, Université Paul Sabatier, 135 Avenue de Rangueil, 31077 Toulouse, France. E-mail: laurent.maron@irsamc.ups-tlse.fr

† Electronic supplementary information (ESI) available. CCDC 2443480–2443489. For ESI and crystallographic data in CIF or other electronic format see DOI: <https://doi.org/10.1039/d5sc03342j>



substituted carbenes (**B1** and **B2**).⁷ Munz *et al.* characterized the Pb species (**C**) as a p-block metallocarbene,⁸ demonstrating that heavier group 14 metalla-alkynes maintain carbene-like reactivity.⁹ Notwithstanding these developments, metallocarbene species continue to be synthetically challenging targets, and their structural and reactive characteristics remain undercharacterized.

The synthesis challenge proves particularly acute for main-group metals with low electronegativity. These obstacles originate primarily from the highly polarized nature of carbon-main-group metal bonds and/or incompatibility in diazo precursor synthesis inherent to Lewis-acidic metal centers. In our previous work, we successfully obtained the first zinc(II) α -diazoalkyl complex.¹⁰ However, the attempt to synthesize the Zn-substituted carbene with this precursor failed, but resulted in the generation of an α -zincated phosphorus ylide due to the presence of a pendant phosphine arm in the ligand framework.

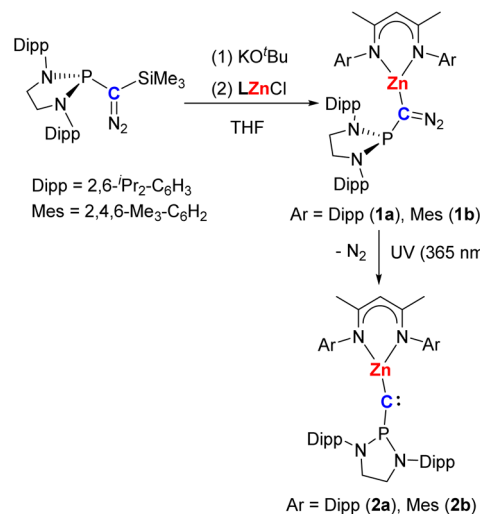
By employing a bidentate β -diketiminato ligand, the successful synthesis of zinc-substituted carbenes was herein achieved *via* photoirradiation of the corresponding diazo precursors (Scheme 1b). Structural analyses revealed their near-linear carbene centers with the notably short Zn–C bond lengths. The resultant Zn-substituted carbene exhibited nucleophilic reactivity toward carbon dioxide (CO_2) with concomitant cleavage of the C=O bond. The unique electrophilic character was demonstrated through the formation of a carbene-Lewis base adduct. Moreover, these metallocarbenes also enabled direct transition metals coordination to afford the heterobimetallic μ -carbyne complexes. The bonding interactions of Zn-substituted carbenes and bimetallic complexes were analyzed using density functional theory (DFT) calculations. This development will be described in this paper.

Results and discussion

Synthesis and characterization of Zn-substituted carbenes

Inspired by the success of the phosphino substituent in stabilizing free carbenes,^{1,11} we initially synthesized two zinc diazoalkyl complexes, each featuring a N-heterocyclic phosphino substituent. They were prepared *via* a two-step one-pot reaction of (phosphino)(silyl)diazomethane, potassium *tert*-butoxide, and the corresponding zinc chlorides LZnCl ($\text{L} = [(\text{ArNCMe})_2\text{CH}]^-$, Ar = 2,6-*i*Pr₂C₆H₃ (**L^a**) or 2,4,6-Me₃C₆H₂ (**L^b**)) in moderate yields (44% for **1a**, 46% for **1b**, Scheme 2). The structures of complexes **1** were confirmed by infrared spectroscopy [$\nu(\text{CN}_2)/\text{cm}^{-1} = 1995$ (**1a**), 2052 (**1b**)], NMR spectroscopy [³¹P{¹H} NMR: 136.4 ppm (**1a**); 128.6 ppm (**1b**)], and X-ray diffraction (Fig. S4 in the ESI†). Treatment of complexes **1** in C₆D₆ under UV irradiation (60 W LED lamp, $\lambda = 365$ nm) afforded the new species quantitatively, corresponding to the significantly upfield-shifted ³¹P{¹H} NMR signals at $\delta = -30.3$ ppm (**2a**) and -16.6 ppm (**2b**), respectively. The reactions were subsequently scaled up in toluene, and gave complexes **2** (88% yield for **2a**, 82% yield for **2b**) as orange crystalline solids (Scheme 2).

Complexes **2** were characterized by single-crystal X-ray diffraction, with the molecular structures depicted in Fig. 1. The Zn–C bond lengths in **2a** [1.871(3) Å] and **2b** [1.847(3) Å] are



Scheme 2 Synthesis of Zn-substituted carbenes 2.

notably shorter than those in the zinc alkyl complex L^aZnEt [1.963(5) Å]¹² and the diazo precursor **1a** [1.954(4) Å], suggesting a stronger Zn–C interaction (*vide infra*). The significantly shortened P–C bond lengths [1.541(3) Å in **2a** and 1.528(3) Å in **2b** vs. 1.832(4) Å in **1a**] and the trigonal planar environment around the P atom in **2** ($\Sigma\text{P}^{\text{CNN}} = 359.8^\circ\text{--}359.9^\circ$) align with enhanced P–C π -interactions, similar to those in phosphinocarbene $\text{Me}_2\text{Si}({}^t\text{Bu}_2)_2\text{PCSiMe}_3$.¹³ The P–C–Zn angle of 163.1(3)° in **2b** is comparable to those of the copper carbyne anion

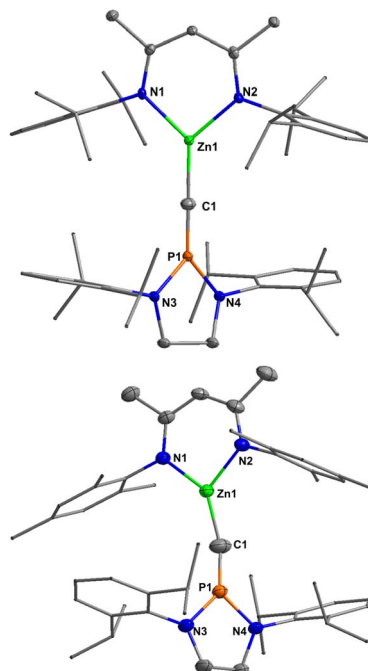


Fig. 1 Molecular structures of carbenes **2a** (top) and **2b** (bottom). Hydrogen atoms are omitted for clarity, and displacement ellipsoids are drawn at the 30% probability level. Aryl groups are drawn in wireframe form.



complex (164.5°)⁶ and the known phosphinocarbenes (131.8 – 162.1°).^{11c} In contrast, the P–C–Zn linkage in **2a** is near-linear [$174.4(2)^\circ$], likely due to the steric repulsion between the Dipp substituents at β -diketiminato ligand and N-heterocyclic phosphino moiety. In solution, the $^{13}\text{C}\{^1\text{H}\}$ NMR resonances of the carbene carbon are located at δ 70.1 ppm ($^1\text{J}_{\text{P}-\text{C}} = 78.5$ Hz) for **2a** and δ 69.7 ppm ($^1\text{J}_{\text{P}-\text{C}} = 25.4$ Hz) for **2b**, respectively.

To gain insights into the bonding situation in complexes **2**, DFT calculations (B3PW91 functional) including dispersion corrections were carried out. The optimized geometry agrees excellently with the experimental data (see Tables S1 and S7 in the ESI†). For complex **2a**, a highly covalent P–C double bond (comprising a σ -bond that is 40% sp on P and 60% sp on C, and a π -bond that is 50% 3p on P and 50% 2p on C) is found at the NBO, while a Zn–C bond is only observed at the second order donor–acceptor level (donation from a sp orbital of C onto the 4s orbital of Zn). The presence of a Zn–C bond is validated by the presence of a Zn–C Bond Critical Point (BCP) in QTAIM. The degree of covalency of the Zn–C and P–C bonds is further highlighted by the Wiberg Bond Index (WBI) values. Indeed, the Zn–C WBI is 0.4 (more than twice that of the Zn–N WBI), consistent with a quite covalent Zn–C interaction. The negative charge on the carbon and the positive charge on the phosphorus suggest that complex **2a** is better described as phosphorus vinyl ylide form, while the P–C WBI of 2.3 supports some contribution of phosphaacylene form as proposed in the copper case.⁶ The situation seems slightly different for complex **2b**. A Zn–C bond is observed at the NBO level, highly polarized toward C (8% 4s of Zn and 92% 2p of C). At the second order donor–acceptor, the remaining C lone pair is delocalized into the Zn–C bond. The selected molecular orbitals of **2b** are shown in Fig. 2a. QTAIM analysis reveals the presence of Zn–C BCP, with a large density value (0.12 vs. 0.06 in **2a**), which is in line with a stronger Zn–C interaction. These features of **2b** support some contribution from the heteroallene form. However, these analyses of complexes **2a** and **2b** clearly show that the different limit structures (Fig. 2b) can easily interconvert, so both

complexes may be viewed as a mixture of these resonance forms.

Reactions of Zn-substituted carbenes with small molecules

Carbene **2a** can be stored at -30°C under a nitrogen atmosphere for weeks without any observed decomposition, whereas it quantitatively converts to a new species **3** upon heating at 80°C in solution (Scheme 3). The molecular structure of complex **3** was authenticated by single-crystal X-ray diffraction (Fig. S21 in the ESI†), revealing carbene C–H insertion at the proximal ^3Pr group, which evidences the nucleophilic character of **2a**.

Carbene-mediated CO_2 activation mode was mostly limited to the formation of corresponding carbene– CO_2 adducts that preserve structural integrity of O–C–O linkage.^{3b} Interestingly, treatment of carbene **2a** in toluene under a CO_2 atmosphere resulted in rapid bleaching and afforded ketene compound **4** *via* a formal C=O double bond cleavage (Scheme 3). The solid structure of **4** (Fig. 3) reveals a significantly elongated P–C bond [$1.764(4)$ Å], suggesting the absence of π -interaction between the P and C atoms. The IR spectrum of **4** shows a very strong C=C=O stretching vibration at 2064 cm^{-1} . The proposed mechanism initiates with nucleophilic attack generating a transient zwitterionic carbene– CO_2 adduct, which subsequently undergoes a Wittig-like intramolecular rearrangement to ultimately afford the zinced (phosphonio)ketene. Such tandem carbene-mediated CO_2 deoxygenation is rarely documented, and was only observed in the reaction of a boryl(phosphino)carbene with CO_2 .¹⁴ Carbene **2b** underwent a similar reaction with CO_2 affording a structurally analogous compound **4b** (See ESI† for details). Additionally, exposure of carbene **2a** to 1 bar CO underwent a formal 1,1-addition to generate complex **5** in 91% isolated yield (Scheme 3). X-ray diffraction analysis (Fig. S32 in the ESI†) reveals that complex **5** adopts a geometric configuration closely resembling that of **4**. Compounds **4** and **5** represent the first examples of zinced ketene derivatives.

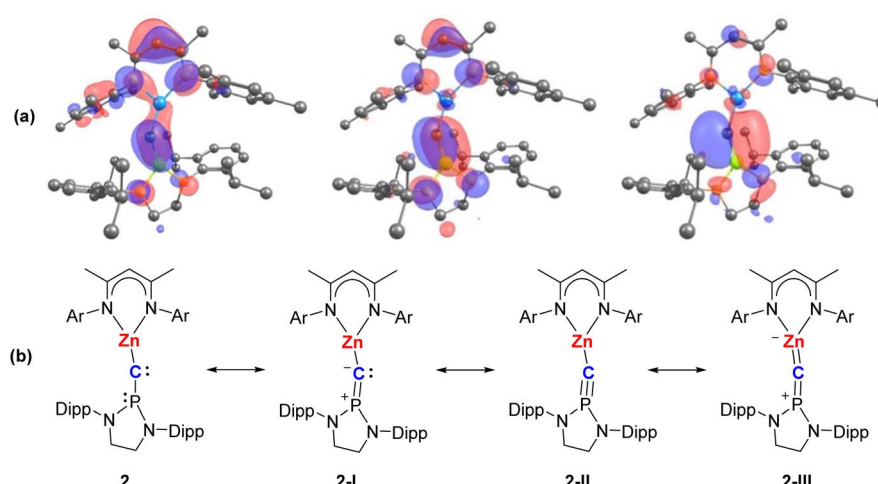
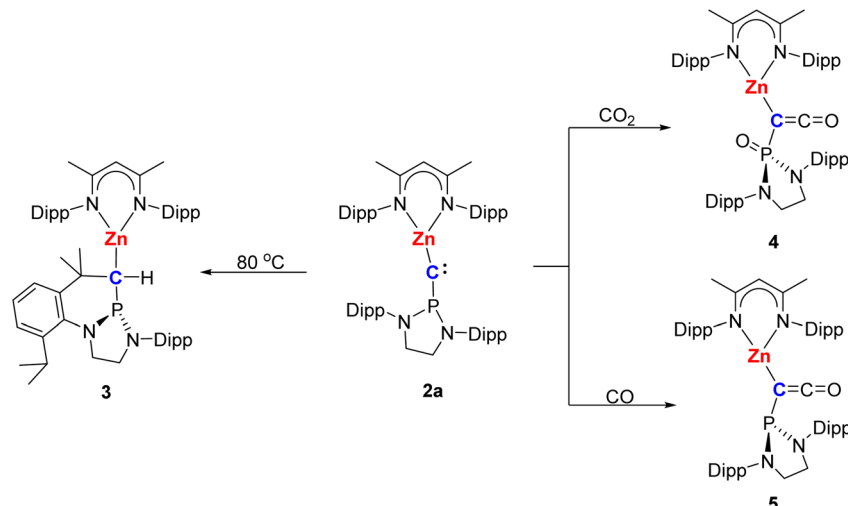


Fig. 2 (a) Selected molecular orbitals of complex **2b**. HOMO-2 (left), HOMO-1 (middle), HOMO (right). (b) The possible resonance structures of **2**.





Scheme 3 Reactivity of 2a leading to 3–5.

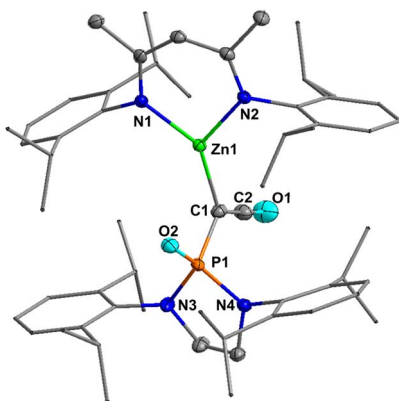


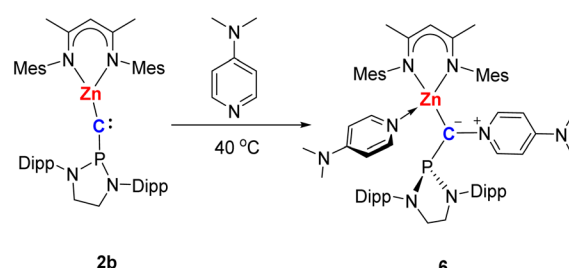
Fig. 3 Molecular structure of 4. Hydrogen atoms are omitted for clarity, and displacement ellipsoids are drawn at the 30% probability level. Aryl groups are drawn in wireframe form.

Carbenes with a unique $p\pi^2$ electronic configuration demonstrate electrophilic character and readily react with Lewis bases to form adducts.¹⁵ In contrast, the stable carbenes with π -donor substituents predominantly exhibit nucleophilic behavior. Notably, the electrophilic carbene character of Zn-substituted carbene 2b was demonstrated by its reaction with 4-dimethylaminopyridine (DMAP). Monitoring the reaction of 2b with DMAP resulted in a gradual color change from light yellow to red, and the carbene-DMAP adduct 6 was isolated as red crystals after workup (Scheme 4). The molecular structure of complex 6 was authenticated by X-ray diffraction (Fig. 4), which shows two molecules of DMAP coordinated to the adjacent carbene and zinc centers, respectively. The carbene carbon center adopts trigonal planar geometry while the phosphino group becomes pyramidalized. The C1–N5 bond length [1.427(6) Å] is slightly shorter than the Pykkö standard value for a C–N single bond (1.46 Å),¹⁶ indicating some ylide character. According to the NBO analysis, the C–N_{DMAP} interaction constitutes a double bond (a σ -bond consisting of 66% sp of N

and 34% sp on C, and a π -bond involving 82% 2p on N and 18% 2p on C), whereas the P–C bond is found to be a single bond (67% sp on C and 33% sp on P). QTAIM analysis indicates the presence of C–N and P–C BCPs with high density, which accounts for the WBI values of C–N and P–C bonds exceeding 1.0 and suggests π -electron delocalization among P, C, and N.

Reactions of Zn-substituted carbenes with transition-metal complexes

Although a few metal-substituted carbenes have been accessed,^{5–8} their feasibility as supporting ligands for constructing heterobimetallic complexes remains undemonstrated. We therefore evaluated Zn-substituted carbenes toward group 10 and 11 metal reagents. The combination of carbene 2a with AgNTf₂ (Tf = SO₂CF₃) successfully gave a heterobimetallic Zn/Ag complex 7. Complex 7 was isolated as a colorless crystalline solid in 85% yield (Scheme 5) and characterized by single-crystal X-ray diffraction as a separated ion pair; the structure of the cation is shown in Fig. 5. The Zn and Ag centers in 7 are bridged by the carbon atom, which adopts a trigonal planar geometry ($\Sigma C^{Zn}P^{Ag} = 359.8^\circ$). The Ag–C bond length is 2.217(6) Å, slightly longer than those in Ag complexes supported by NHCs [av. 2.12(1) Å].¹⁷ The Zn–Ag and P–Ag distances in 7 are 3.1990(7) and 2.9563(14) Å, respectively, which are significantly longer than the corresponding sums of the covalent radii



Scheme 4 Synthesis of complex 6.

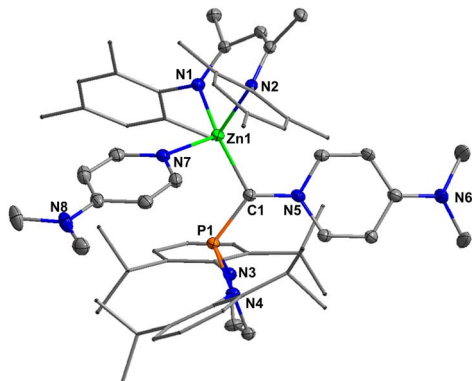


Fig. 4 Molecular structure of **6**. Hydrogen atoms are omitted for clarity, and displacement ellipsoids are drawn at the 30% probability level. Aryl groups are drawn in wireframe form.

(Alvarez radii, Zn–Ag: 2.67 Å; P–Ag: 2.52 Å;¹⁸ Pykko radii, Zn–Ag: 2.46 Å; P–Ag: 2.39 Å¹⁶), ruling out possible Zn/P–Ag interaction. This is also corroborated by a $^{31}\text{P}\{^1\text{H}\}$ NMR singlet at δ 55.3 ppm in solution, with no observed Ag–P coupling. The planarization of the phosphino group ($\Sigma\text{P}^{\text{NNC}} = 360.0^\circ$) and short P–C bond length [1.584(6) Å] reveal the presence of P \rightarrow C π -donation. While cationic silver(i) complex typically adopts linear two-coordinate geometry, complex **7** unexpectedly manifests a mono-substituted Ag⁺ center stabilized *via* arene π -interactions with two eclipsed Dipp groups. The bonding analysis by DFT shows a Ag–C bond in **7**, which is strongly polarized toward the C atom (89%). Its BCP and WBI are similar to those of the Zn–C bond, indicating single bond character. The P–C BCP has the highest density, and its WBI is 1.6, consistent with a reduced but remaining π -interaction.

An analogous reaction also occurred with the gold reagent $\text{Au}(\text{PPh}_3)\text{NTf}_2$, generating Zn/Au complex **8** in 98% yield (Scheme 5). The molecular structure of **8** determined by X-ray diffraction is provided in the ESI (Fig. S46).[†] The Au–C bond length of 2.052(5) Å is slightly longer than that in Au-substituted

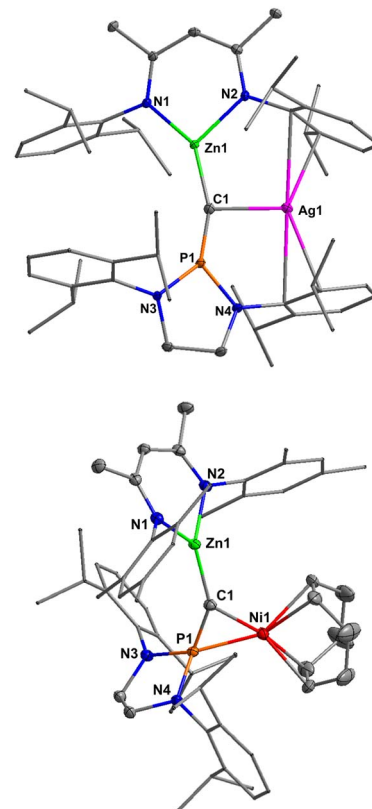
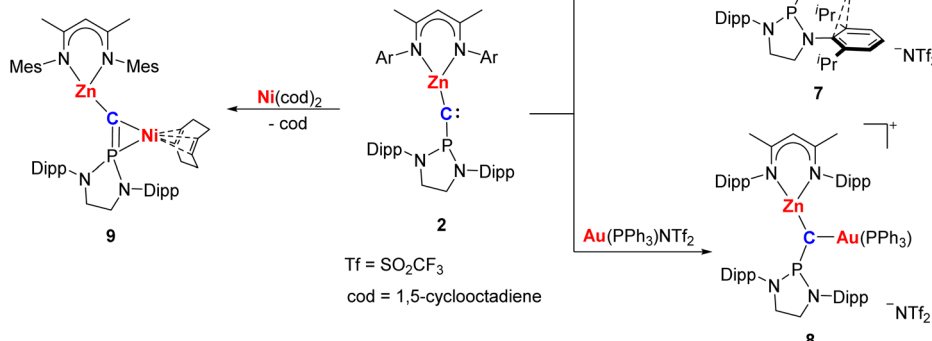


Fig. 5 Molecular structures of **7** (top) and **9** (bottom). Hydrogen atoms and NTf_2^- anion in **7** are omitted for clarity, and displacement ellipsoids are drawn at the 30% probability level. Aryl groups are drawn in wireframe form.

carbene species [1.945(3) Å]⁵ but comparable to the values in cationic gold carbene complexes.¹⁹ Noteworthily, although μ -carbyne complexes of high-spin transition metals are well-documented,²⁰ analogous complexes involving closed-shell d¹⁰ metal fragments remain scarce. Complexes **7** and **8** represent



Scheme 5 Reactions of Zn-substituted carbenes **2** with transition-metal reagents.



rare examples of μ -carbyne complexes exclusively comprising d^{10} metal fragments.

The reaction of carbene **2b** with $\text{Ni}(\text{cod})_2$ (cod: 1,5-cyclooctadiene) at 60 °C yielded the heterobimetallic Zn/Ni complex **9** in 79% isolated yield (Scheme 5). Red crystals of **9** suitable for X-ray diffraction were obtained from a hexane solution at –30 °C and the molecular structure is shown in Fig. 5. Different from **7** and **8**, the Zn-substituted carbene framework in complex **9** serves as an η^2 -ligand at Ni center featuring a three-membered metallocycle [Ni1-C1 1.920(3) , $\text{Ni1-P1 2.1350(8) \AA}$], in line with the established bonding modes in phosphinocarbene transition metal complexes.²¹ The P–C bond lengthens to 1.643(3) Å, indicating the reduce of P–C π -interaction. Thus, the C–P fragment can be interpreted as a λ^5 -phosphaalkyne ligand.^{4a} The NBO analysis for complex **9** indicated some double bond character between C and Ni, which is found only at the second order donor–acceptor level (donation from 2p lone pair on C onto the mostly 4s orbital of Ni and donation from an sp lone pair on C onto the antibonding Ni–P bond). This is further corroborated by the QTAIM analysis, which reveals a Ni–C BCP with high electron density.

Conclusions

The synthesis of zinc-substituted carbenes was successfully achieved *via* irradiation of the β -diketiminato ligand-supported zinc diazoalkyl complexes. Bonding analysis confirms the resultant species as singlet carbenes stabilized by C–P π -interaction. The reactivity of these complexes was comprehensively investigated, revealing their ambiphilic carbene nature. The observed C–H and C=O bond cleavages demonstrated nucleophilic character, while the electrophilic behaviour was verified by the formation of a carbene–Lewis base adduct. Intriguingly, three heterometallic complexes were facilely obtained by the coordination of Zn-substituted carbenes to the corresponding transition-metal reagents. The silver and gold complexes represent two novel μ -carbyne complexes involving exclusively d^{10} metal fragments. The potential of these complexes in catalysis is currently under active investigation in our laboratory.

Data availability

For synthetic procedures, analytic data, full descriptions of the methods and details of the DFT calculations contained in this paper see ESI.†

Author contributions

X. X. conceived and supervised the study. S. J. and Y. C. performed the experiments and analyzed the data. L. M. and G. W. performed the computational studies. S. J., L. M. and X. X. wrote the paper. All authors have read and proofed the paper.

Conflicts of interest

There are no conflicts to declare.

Acknowledgements

This work was supported by the National Natural Science Foundation of China (22301203, 22371198) and the Jiangsu Funding Program for Excellent Postdoctoral Talent (2023ZB771). LM is a senior member of the Institut Universitaire de France. CalMip is acknowledged for a generous grant of computing time. The Chinese Scholarship Council (CSC) is acknowledged for financial support (PhD grant of G. W.).

References

- 1 A. Igau, H. Grutzmacher, A. Baceiredo and G. Bertrand, *J. Am. Chem. Soc.*, 1988, **110**, 6463–6466.
- 2 A. J. Arduengo III, R. L. Harlow and M. Kline, *J. Am. Chem. Soc.*, 1991, **113**, 361–363.
- 3 (a) S. Diez-González, N. Marion and S. P. Nolan, *Chem. Rev.*, 2009, **109**, 3612–3676; (b) V. Nesterov, D. Reiter, P. Bag, P. Frisch, R. Holzner, A. Porzelt and S. Inoue, *Chem. Rev.*, 2018, **118**, 9678–9842; (c) T. Koike, J.-K. Yu and M. M. Hansmann, *Science*, 2024, **385**, 305–311.
- 4 (a) D. Bourissou, O. Guerret, F. P. Gabbaï and G. Bertrand, *Chem. Rev.*, 2000, **100**, 39–92; (b) J. Vignolle, X. Cattoën and D. Bourissou, *Chem. Rev.*, 2009, **109**, 3333–3384.
- 5 C. Hu, X.-F. Wang, R. Wei, C. Hu, D. A. Ruiz, X.-Y. Chang and L. L. Liu, *Chem.*, 2022, **8**, 2278–2289.
- 6 R. Wei, X.-F. Wang, C. Hu and L. L. Liu, *Nat. Synth.*, 2023, **2**, 357–363.
- 7 (a) Z.-J. Lv, K. A. Eisenlohr, R. Naumann, T. Reuter, H. Verplancke, S. Demeshko, R. Herbst-Irmer, K. Heinze, M. C. Holthausen and S. Schneider, *Nat. Chem.*, 2024, **16**, 1788–1793; (b) Z.-J. Lv, A. Fitterer, R. Herbst-Irmer, S. Demeshko, H. Verplancke, M. C. Holthausen and S. Schneider, *J. Am. Chem. Soc.*, 2025, **147**, 5590–5595.
- 8 F. Dankert, J. Messelberger, U. Authesserre, A. Swain, D. Scheschkewitz, B. Morgenstern and D. Munz, *J. Am. Chem. Soc.*, 2024, **146**, 29630–29636.
- 9 (a) X.-F. Wang, C. Hu, J. Li, R. Wei, X. Zhang and L. L. Liu, *Nat. Chem.*, 2024, **16**, 1673–1679; (b) R. Wei, X.-F. Wang, C. Hu and L. L. Liu, *Chem. Commun.*, 2024, **60**, 9793–9796; (c) X.-F. Wang, C. Hu, Z. Lu and L. L. Liu, *Sci. China Chem.*, 2024, **67**, 4212–4217.
- 10 S. Jiang, Y. Cai, T. Rajeshkumar, I. Del Rosal, L. Maron and X. Xu, *Angew. Chem., Int. Ed.*, 2023, **62**, e202307244.
- 11 (a) C. Buron, H. Gornitzka, V. Romanenko and G. Bertrand, *Science*, 2000, **288**, 834–836; (b) L. Liu, D. A. Ruiz, D. Munz and G. Bertrand, *Chem.*, 2016, **1**, 147–153; (c) C. Hu, X. F. Wang, C. Hu, R. Wei, H. Wang and L. L. Liu, *Acc. Chem. Res.*, 2025, **58**, 452–462; (d) R. Wei, F. Huang, X. Lan, Q. Liang and L. L. Liu, *Chin. J. Chem.*, 2025, **43**, 1547–1552.
- 12 M. Cheng, D. R. Moore, J. J. Reczek, B. M. Chamberlain, E. B. Lobkovsky and G. W. Coates, *J. Am. Chem. Soc.*, 2001, **123**, 8738–8749.
- 13 T. Kato, H. Gornitzka, A. Baceiredo, A. Savin and G. Bertrand, *J. Am. Chem. Soc.*, 2000, **122**, 998–999.



14 F. Lavigne, E. Maerten, G. Alcaraz, V. Branchadell, N. Saffon-Merceron and A. Baceiredo, *Angew. Chem., Int. Ed.*, 2012, **51**, 2489–2491.

15 (a) J. Ruiz, M. E. G. Mosquera, G. García, E. Patrón, V. Riera, S. García-Granda and F. Van der Maelen, *Angew. Chem., Int. Ed.*, 2003, **42**, 4767–4771; (b) J. Vignolle, H. Gornitzka, L. Maron, W. W. Schoeller, D. Bourissou and G. Bertrand, *J. Am. Chem. Soc.*, 2007, **129**, 978–985; (c) Y. Shibutani, S. Kusumoto and K. Nozaki, *J. Am. Chem. Soc.*, 2023, **145**, 16186–16192; (d) C. Hu, X.-F. Wang, J. Li, X.-Y. Chang and L. L. Liu, *Science*, 2024, **383**, 81–85.

16 P. Pyykkö, *J. Phys. Chem. A*, 2014, **119**, 2326–2337.

17 J. C. Garrison and W. J. Youngs, *Chem. Rev.*, 2005, **105**, 3978–4008.

18 B. Cordero, V. Gómez, A. E. Platero-Prats, M. Revés, J. Echeverría, E. Cremades, F. Barragán and S. Alvarez, *Dalton Trans.*, 2008, 2832–2838.

19 (a) H. G. Raubenheimer and S. Cronje, *Chem. Soc. Rev.*, 2008, **37**, 1998–2011; (b) M. Navarro and D. Bourissou, in *Advances in Organometallic Chemistry*, ed. P. J. Pérez, Academic Press, 2021, vol. 76, pp. 101–144.

20 X. Zhai, M. Xue, Q. Zhao, Q. Zheng, D. Song, C. H. Tung and W. Wang, *Nat. Commun.*, 2024, **15**, 7729.

21 (a) E. Despagnet, K. Miqueu, H. Gornitzka, P. W. Dyer, D. Bourissou and G. Bertrand, *J. Am. Chem. Soc.*, 2002, **124**, 11834–11835; (b) K. Miqueu, E. Despagnet-Ayoub, P. W. Dyer, D. Bourissou and G. Bertrand, *Chem.-Eur. J.*, 2003, **9**, 5858–5864.

